JOURNAL OF MATERIALS SCIENCE 20 (1985) 4421–4430

Direct measurements of non-linear stress–strain curves and elastic properties of metal matrix composite sandwich beams with any core material

JACQUES E. SCHOUTENS
Metal Matrix Composite Information Analysis Center, Kaman Tempo, 816 State Street, Santa Barbara, California 93102, USA

A theory for measuring non-linear stress–strain curves and elastic properties of metal matrix composite (MMC) sandwich beams subjected to pure bending loads is discussed. The beam is made from any core material sandwiched between an upper facing of unreinforced metal and a lower facing of MMC with unidirectional fibre reinforcement or vice versa. The model developed shows that the determination of the position of the neutral axis is critical to the measurements discussed in this paper. The analysis removes the restriction of the effects of the core. With the aid of this model, we show that the position of the neutral axis can be determined directly from surface strain measurements. Measurements of neutral axis position lead directly to the determination of the beam elastic properties and, thus, directly obtained from surface strain measurements. It is shown that the model predicts longitudinal stresses and strains within any layer of the beam. The analysis includes the limiting case of a very weak core material. A consequence of this model is the determination of the MMC facing fibre volume fraction. A detailed error analysis predicts that the longitudinal elastic modulus of an MMC material facing can be obtained with an uncertainty between 4 and 6% if the surface strain measurements and beam dimensions can be obtained with an uncertainty of 1%. The volume fraction can be obtained within 10% uncertainty, although better methods are available for that measurement.

1. Introduction

In the pure bending of sandwich beams, the axial stiffness of the core material in tension or compression is usually considered to be negligible compared with the stiffness of the facing materials. To meet the requirement of weak core material, cores are generally made from relatively large prismatic hexagonal cells of aluminium foil or paper, with the prismatic cell axis perpendicular to the facings. Such an analysis also assumes that the core bonding to the facing is perfect. These restrictions result in simple models for obtaining stress–strain curves from surface strain measurements. The model proposed by Bert [1] is such a simple model, although it predicts compressive strains in the centre of the compressed facing material which are greater than the surface strain! Generally, elastic properties obtained from bending tests yield values that are somewhat higher than from tensile tests.

There are conditions in which the sandwich beam whose mechanical properties are desired consists of a stiff core with only marginally stiffer facing materials. This is the case treated in this paper. The present treatment effectively removes the weak core assumption and predicts sandwich beam mechanical properties in the

0022–2461/85 $03.00 + .12

limit of very weak core material. In the present analysis, the sandwich beam is assumed to be made from any core material and any facing material. Thus, the core can be made from low stiffness metal, porous material, or resins. Because of their low ductility, dense ceramics sandwich beam materials may have to be analysed by other methods. To obtain meaningful mechanical properties for sandwich beams with any core materials, the test specimen should have a large span-to-depth ratio to minimize the effects of shear deformation [2]. Thus, in the following analysis, a beam cross-section is assumed to remain planar during bending.

2. Analysis

Fig. 1 shows the cross-section of a sandwich beam of width W and total thickness H. It consists of three materials: a top facing having an elastic modulus, E_m; a core material with an elastic modulus, E_l; and a bottom facing material made of unidirectional fibre reinforced MMC of longitudinal modulus, E_c. We assume that $E_l \lesssim E_m$ and $E_m \lesssim E_c$. This means that the neutral axis will be at the sandwich beam centre line or below it by a fractional value α. (It will be above the centre line if the stiffer facing is at the top.) The top facing has thickness t_u and the bottom facing thickness t_b. A bending moment M is applied to the beam as shown, resulting in the material above the neutral axis being in compression and that below it being in tension. The compressive stress in the centre of the upper facing is σ_c, and in the centre of the bottom facing it is σ_t. The compressive and tensile stresses in the core material are σ_{cm} and σ_{tm}, respectively. The upper facing has area A_u, the bottom facing area is A_b, and the compressive and tensile regions of the core areas are A_{um} and A_{bm}, respectively, these areas depending on the position of the neutral axis. The positions of these stresses with respect to the neutral axis are given by

$$a = \tfrac{1}{2}[(1 + \alpha)H - t_u] \quad (1)$$

$$b = \tfrac{1}{3}[(1 + \alpha)H - 2t_u] \quad (2)$$

$$c = \tfrac{1}{3}[(1 - \alpha)H - 2t_b] \quad (3)$$

$$d = \tfrac{1}{2}[(1 - \alpha)H - t_b] \quad (4)$$

and the areas are

$$A_u = t_u W \quad (5)$$

$$A_{um} = \tfrac{1}{2}[(1 + \alpha)H - 2t_u]W \quad (6)$$

$$A_{bm} = \tfrac{1}{2}[(1 - \alpha)H - 2t_b]W \quad (7)$$

$$A_b = t_b W \quad (8)$$

and the linear stresses (Hooke's Law behaviour) are given by

$$\sigma_c = -\frac{a}{r}E_m = -\frac{E_m}{2r}[(1 + \alpha)H - t_u] \quad (9)$$

$$\sigma_{cm} = -\frac{b}{r}E_l = -\frac{E_l}{3r}[(1 + \alpha)H - 2t_u] \quad (10)$$

$$\sigma_{tm} = \frac{c}{r}E_l = \frac{E_l}{3r}[(1 - \alpha)H - 2t_b] \quad (11)$$

$$\sigma_t = \frac{d}{r}E_c = \frac{E_c}{2r}[(1 - \alpha)H - t_b] \quad (12)$$

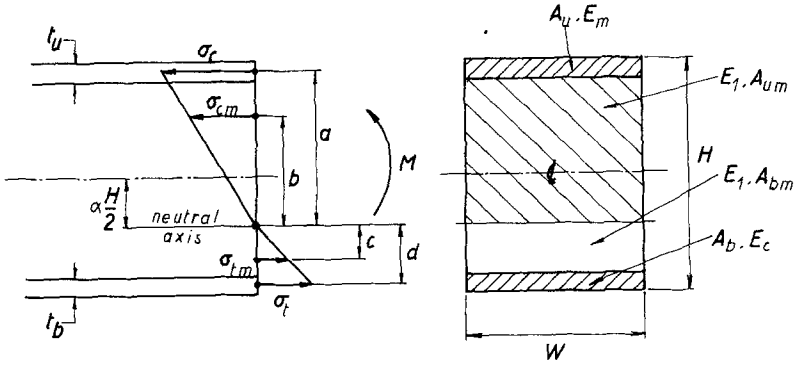

Figure 1 Schematic illustration of sandwich beam-stress diagram used in the present analysis.

where r is the radius of curvature of the neutral axis. The sum of forces acting upon the cross-section is given by

$$\sigma_c A_u + \sigma_{cm} A_{um} + \sigma_{tm} A_{bm} + \sigma_t A_b = 0 \quad (13)$$

Substituting Equations 1 to 12 into Equation 13 yields the position of the neutral axis, after considerable algebra, as

$$\alpha = \frac{4E_l[(t_u^2 - t_b^2) - (t_u - t_b)H] + 3E_m(Ht_u - t_u^2) + 3E_c(t_b^2 - Ht_b)}{(4E_l - 3E_m)Ht_u - (3E_c - 4E_l)Ht_b - 4E_l H^2} \quad (14)$$

Note that in this derivation, the neutral axis was assumed to be below the beam centre line because the bottom facing tensile strength and stiffness were assumed greater than that of the top facing. In the reverse case, $\alpha < 0$.

2.1. Case for equal facing thickness and strong core

When $t_u = t_b = t$ is assumed, then the general case given by Equation 14 reduces to

$$\alpha_1 = \frac{3(E_c - E_m)(1 - t/H)}{8E_l(H/2t - 1) + 3(E_c + E_m)} \quad (15)$$

which shows the influence of the core stiffness on the location of the neutral axis. Now, the effects of the core can be determined somewhat more easily by using the following definition

$$E_l = fE_m \quad (16)$$

where f is a fraction whose value can range between close to zero and unity or $0 \lesssim f \leqslant 1$. Then we find that Equation 15 becomes

$$\alpha_2 = \frac{3(E_c - E_m)(1 - t/H)}{[8f(H/2t - 1) + 3]E_m + 3E_c} \quad (17)$$

This approach is seen to be useful later.

2.2. Case for a weak core

Again, considering that $t_u = t_b = t$ in Equation 14 and assuming that a weak core can be simulated by setting $f \simeq 0$, Equation 14 can be reduced to

$$\alpha_3 = \frac{E_c - E_m}{E_c + E_m}\left(1 - \frac{t}{H}\right) \quad (18)$$

This equation clearly shows that when $E_c = E_m$, $\alpha = 0$, or the neutral axis is at the centre line of the beam cross-section.

In the above equation, it can be seen also that when $t_u \to H$ or $t_b \to H$ or the entire core thickness becomes H, then $\alpha = \alpha_1 = \alpha_2 = \alpha_3 = 0$ as it should. Likewise, when $E_c = E_m = E_l = E$, then $\alpha = \alpha_1 = \alpha_2 = \alpha_3 = 0$.

2.3. Parametric case for MMC

When $t_u = t_b = t$, we can consider another simplifying approach. The longitudinal elastic modulus of a unidirectional fibre reinforced MMC facing material can be obtained, to a good approximation, from the rule of mixtures

$$E_c = E_f V_f + (1 - V_f)E_m \quad (19)$$

where V_f is the volume fraction of fibre in the composite, and using a definition employed elsewhere [3],

$$E_f = K_0 E_m \quad (20)$$

where K_0 is a constant. Equation 19 can then be written as

$$E_c = \{(K_0 - 1)V_f + 1\}E_m \quad (21)$$

For a strong core case, substituting Equation 21 into Equation 17 yields

$$\alpha_2 = \frac{3(K_0 - 1)V_f(1 - t/H)}{8f(H/2t - 1) + 3(K_0 - 1)V_f + 6} \quad (22)$$

Thus, $\alpha_2 = \alpha_2(K_0, V_f, t, H)$ and can be parameterized in design analyses for cases where the neutral axis positions are needed. Note that as $K_0 \to 1$ ($V_f \to 0$ [3]), then $\alpha_2 \to 0$. For a weak core when $f \simeq 0$, Equation 22 reduces to

$$\alpha_3 = \frac{(K_0 - 1)V_f}{(K_0 - 1)V_f + 2}\left(1 - \frac{t}{H}\right). \quad (23)$$

Table I summarizes the expressions for the position of the neutral axis so far derived.

2.4. Linear stress relations

The linear or Hooke Law stress relations can be derived from Equations 1 to 13 and a sum of moments about the neutral axis, or

$$M = \sigma_c A_u a + \sigma_{cm} A_{um} b + \sigma_{tm} A_{bm} c + \sigma_t A_b d. \quad (24)$$

Substituting Equations 5 to 8 into Equation 24 yields

$$M = W\{\sigma_c t_u a + \tfrac{3}{2}\sigma_{cm} b^2 + \tfrac{3}{2}\sigma_{tm} c^2 + \sigma_t t_b d\}. \quad (25)$$

TABLE I Summary of the expressions for the position of the neutral axis

Parameters	α	Comments
$t_u \neq t_b$, H $E_l \neq E_m \neq E_c$	$\frac{4E_l[(t_u^2 - t_b^2) - (t_u - t_b)H] + 3E_m(Ht_u - t_u^2) + 3E_c(t_b^2 - Ht_b)}{(4E_l - 3E_m)Ht_u - (3E_c - 4E_l)Ht_b - 4E_lH^2}$	General case (Equation 14)
$t_u = t_b = t$ $E_c > E_m > E_l$	$\frac{3(E_c - E_m)(1 - t/H)}{8E_l(H/2t - 1) + 3(E_c + E_m)}$	Strong core (Equation 15)
$t_u = t_b = t$ $E_c > E_m$, $E_l = fE_m$ $0 \lesssim f \leqslant 1$	$\frac{3(E_c - E_m)(1 - t/H)}{[8f(H/2t - 1) + 3]E_m + 3E_c}$	Strong core (Equation 17)
$t_u = t_b = t$ $E_l \ll E_m$ or E_c $f \simeq 0$	$\frac{E_c - E_m}{E_c + E_m}\left(1 - \frac{t}{H}\right)$	Weak core (Equation 18)
$t_u = t_b = t$ $E_f = K_0E_m$, $E_l = fE_m$ $f \neq 0$, $E_c > E_m$	$\frac{3(K_0 - 1)V_f(1 - t/H)}{8f(H/2t - 1) + 3(K_0 - 1)V_f + 6}$	Strong core parametric case (Equation 22)
$t_u = t_b = t$ $E_l \ll E_m$ or E_c, $f \simeq 0$ $E_f = K_0E_m$	$\frac{(K_0 - 1)V_f}{(K_0 - 1)V_f + 2}\left(1 - \frac{t}{H}\right)$	Weak core parametric case (Equation 23)

Now, from the stress diagram in Fig. 1, we note that

$$\frac{\sigma_c}{a} = \frac{\sigma_{cm}}{b} \tag{26}$$

and

$$\frac{\sigma_t}{d} = \frac{\sigma_{tm}}{c} \tag{27}$$

and eliminating σ_{cm} and σ_{tm} in Equation 25 using Equations 26 and 27 yields

$$\sigma_c = -\frac{d}{a}\left[t_b + \frac{3}{2}\frac{c^3}{d^2}\right]\Big/\left[t_u + \frac{3}{2}\frac{b^3}{a^2}\right]\sigma_t$$
$$= -A\sigma_t \tag{28}$$

and substituting Equation 28 into the moment Equation 25 gives, after some algebra, that the tensile stress in the centre of the bottom facing is given by

$$\sigma_t = \frac{4adM}{W[2a(2d^2t_b + 3c^3) - 2d(2a^2t_u + 3b^3)A_0]} \tag{29}$$

where a, b, c, and d are given by Equations 1 to 4, and

$$A_0 = \frac{a}{d}\left(\frac{2d^2t_b + 3c^3}{2a^2t_u + 3b^3}\right) \tag{30}$$

Equation 30 is the same as Equation 28 defining A. Equations 28 and 29 give the stresses at the centre of the facings in terms of the bending moment for the case of a strong core. Since a, b, c, and d are functions of α, σ_t and σ_c are also functions of α. The value of α can be either calculated as shown by the equations listed in Table I, or can be measured, as we will discuss below. In the special case when $t_u = t_b = t$, Equations 29 and 30 remain unchanged except for that substitution. For a weak core, the compressive and tensile stresses can be neglected in the core compared to the facing material strength, so that the moment equation becomes

$$M_w \simeq (\sigma_c t_u a + \sigma_t t_d d)\, W \tag{31}$$

where the sign $\simeq$ is set because $f \simeq 0$, and the force equation becomes

$$\sigma_c t_u W + \sigma_t t_b W \simeq 0 \tag{32}$$

Eliminating σ_c between Equations 31 and 32 yields

$$\sigma_t = \frac{2M}{(t_u - t_b - 2\alpha H)t_b} \tag{33}$$

and eliminating σ_t in Equations 31 and 32 yields

$$\sigma_c = -\frac{2M}{(t_u - t_b - 2\alpha H)t_u} \tag{34}$$

These equations give the linear stress relation in the centre of the facing material with the assumption that the core material exerts a negligible effect upon these facings other than for stability against buckling.

2.5. Strain relations

Fig. 2 shows a diagram for computing the strain relations. The compressive surface strain at the top facing is ε_{cu} and the tensile surface strain at the bottom facing is ε_{tb}. These strains are a distance a_u and a_b, respectively, from the neutral axis, given by

$$a_u = \tfrac{1}{2}(1 + \alpha)H \quad (35)$$

$$a_b = \tfrac{1}{2}(1 - \alpha)H \quad (36)$$

and compressive and tensile strains anywhere within layers parallel to the sandwich beam faces are given by

$$\varepsilon_c = \frac{y_u}{a_u}\varepsilon_{cu} \quad (37)$$

for compressive strains, and

$$\varepsilon_t = \frac{y_b}{a_b}\varepsilon_{tb} \quad (38)$$

for the tensile strains. Substitution of Equations 35 and 36 into Equations 37 and 38 immediately yields

$$\varepsilon_c = \frac{2\varepsilon_{cu}}{(1 + \alpha)H} y_u \quad (39)$$

and

$$\varepsilon_t = \frac{2\varepsilon_{tb}}{(1 - \alpha)H} y_b \quad (40)$$

and when $\alpha = 0$, which implies facing materials of equal stiffnesses, $\varepsilon_{tb} = \varepsilon_{cu}$ so that $\varepsilon_c = 2\varepsilon_{cu}y_u/H$ and $\varepsilon_t = 2\varepsilon_{tb}y_b/H$. Now we can calculate the strain in the centre of the facing materials. For the top face, $y_u \equiv a$ given by Equation 1, so that by substitution into Equation 39, there results

$$\varepsilon_c = \varepsilon_{cu}\left[1 - \left(1 + \frac{\varepsilon_{tb}}{\varepsilon_{cu}}\right)\frac{t_u}{2H}\right] \quad (41)$$

and for the tensile strain in the centre of the bottom facing, with $y_b \equiv b$ given by Equation 2, there results

$$\varepsilon_t = \varepsilon_{tb}\left[1 - \left(1 + \frac{\varepsilon_{cu}}{\varepsilon_{tb}}\right)\frac{t_b}{2H}\right] \quad (42)$$

These equations show that these strains are obtained entirely from measured quantities: surface strains and sandwich beam dimensions. Moreover, these strains are independent of the core material in this model. A simple analysis shows that in the case of facing material of equal thickness, Equations 41 and 42 reduce to

$$\varepsilon_c = \varepsilon_{cu}\left(1 - \frac{t_u}{H}\right) \quad (43)$$

for the compressive strain, and for the tensile strain

$$\varepsilon_t = \varepsilon_{tb}\left(1 - \frac{t_b}{H}\right) \quad (44)$$

The surface strains can now be related to the radius of curvature of the neutral axis in the following manner. The surface compressive strain [4] is given by

$$\varepsilon_{cu} = -(1 + \alpha)\frac{H}{2r} \quad (45)$$

and the surface tensile strain is given by

$$\varepsilon_{tb} = (1 - \alpha)\frac{H}{2r} \quad (46)$$

where r is the radius of curvature. Taking the absolute value of ε_{cu} in Equation 45, solving that equation and Equation 46 for the radius of curvature, and equating the results and solving for α, we obtain what can be considered the measured position of the neutral axis, α_m, or

$$\alpha_m = \frac{\varepsilon_{cu} - \varepsilon_{tb}}{\varepsilon_{cu} + \varepsilon_{tb}} \quad (47)$$

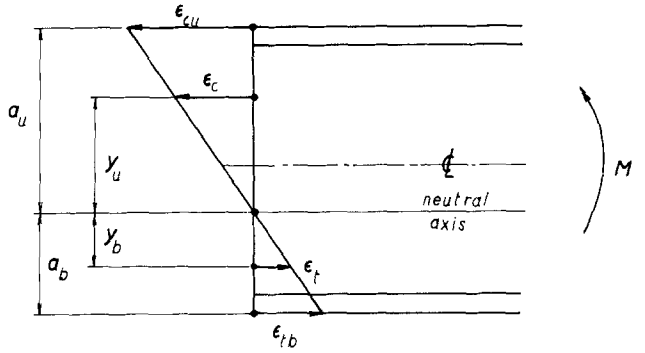

Figure 2 Diagram for computing strain relations.

which shows that it depends only on measured surface strains. This is, of course, a consequence of the model employed.

3. Measurements of mechanical properties

We have shown above that the strains within a sandwich beam, as shown in Fig. 1, can be obtained from surface strain measurements and beam dimensions, and that the neutral axis can be obtained also from surface strain measurements. The position of the neutral axis from surface strain measurements is based on the assumption that shear deformation of any beam cross-section is entirely negligible. Using Equation 47, we can develop an expression for the MMC facing material elastic modulus. This analysis applies to any facing material, top or bottom. Equation 17 gives the neutral axis position for the case of a strong core. Equating Equations 17 and 47 gives

$$\frac{\varepsilon_{cu} - \varepsilon_{tb}}{\varepsilon_{cu} + \varepsilon_{tb}} = \frac{3(E_c - E_m)(2 - t/H)}{[8f(H/2t - 1) + 3]E_m + 3E_c} \quad (48)$$

which, when solved for E_c, after considerable algebra, gives

$$E_c = \left[\frac{8fH(H - 2t)(\varepsilon_{tb} - \varepsilon_{cu}) + 12t^2(\varepsilon_{tb} + \varepsilon_{cu}) - 24Ht\varepsilon_{cu}}{12t^2(\varepsilon_{cu} + \varepsilon_{tb}) - 24Ht\varepsilon_{tb}}\right] E_m \quad (49)$$

This equation shows that E_c is obtained from surface strain and beam dimension measurements only. In the next section, we will discuss the uncertainties in such measurements. Equation 49 is for the strong core material case.

When the core material is weak, then Equation 18 is equated to Equation 47 to yield

$$\frac{\varepsilon_{cu} - \varepsilon_{tb}}{\varepsilon_{cu} + \varepsilon_{tb}} = \frac{E_c - E_m}{E_c + E_m}\left(1 - \frac{t}{H}\right) \quad (50)$$

which, when solved for E_c, gives

$$E_c = \frac{\varepsilon_{cu} - (\varepsilon_{cu} + \varepsilon_{tb})(t/2H)}{\varepsilon_{tb} - (\varepsilon_{cu} + \varepsilon_{tb})(t/2H)} E_m \quad (51)$$

Equation 49 reduces to Equation 51 when $f \simeq 0$. In Equations 49 and 50, it is assumed that the top and bottom facings have identical thicknesses or $t_u = t_b = t$. To obtain the general case for different facing material thicknesses and a strong core, Equations 14 and 47 must be equated and solved for E_c. This is not so much a complex problem as a tedious one, involving considerable algebraic manipulation. We restricted the present analysis to equal facing thicknesses because better insights can be obtained into the consequences of the model with rather minor restrictions ($t_u = t_b = t$). Equations 49 and 51 reduce to $E_c = E_m$ when $\alpha = 0$ which means the case of identical facing materials. Therefore, it is only possible to obtain elastic properties of an MMC facing material if the other facing material exhibits a known but different elastic modulus, regardless of the core material used.

3.1. Measurement of fibre volume fraction

The model developed so far implies that it may be possible to obtain the fibre volume fraction of the composite material facing. Equations 22 and 23 give the position of the neutral axis for the cases of a strong and a weak core, respectively. These expressions are parametric in V_f and $K_0 = E_f/E_m$, which is convenient for design analyses [3]. Therefore, these equations lend themselves to calculating V_f. After a lot of algebra, equating Equations 22 and 47 and solving for V_f gives the volume fraction of the composite facing for the strong core case as

$$V_f = \frac{H[8f(H/2t - 1) + 6](\varepsilon_{tb} - \varepsilon_{cu})}{3(K_0 - 1)[(\varepsilon_{cu} + \varepsilon_{tb})t - 2H\varepsilon_{tb}]} \quad (52)$$

and equating Equation 23 to Equation 47 and solving for V_f gives for the weak core case

$$V_f = \frac{2(\varepsilon_{tb} - \varepsilon_{cu})}{[(2 - K_0)\varepsilon_{cu} - K_0\varepsilon_{tb}](1 - t/H)} \quad (53)$$

In these derivations, again we have assumed $t_u = t_b = t$. We see that in both the strong and weak core cases, V_f depends only on the sandwich beam dimensions and the measured surface strains, and the ratio of the measured fibre-to-matrix elastic modulus.

4. Error analysis

The equations derived in the preceding sections can be represented by functional relationships of the form $f = f(x_1, x_2, x_3, \ldots)$ where x_1, x_2, x_3, . . . are measured quantities. In estimating

the errors in the values of x_1, x_2, x_3, . . . , the cross-correlation terms are neglected and, therefore, covariant uncertainities are not considered. Consequently, the uncertainty in this functional relationship can be written as [5]

$$\Delta f^2 = \left(\frac{\partial f}{\partial x_1}\right)^2 \Delta x_1^2 + \left(\frac{\partial f}{\partial x_2}\right)^2 \Delta x_2^2 + \left(\frac{\partial f}{\partial x_3}\right)^2 \Delta x_3^2 + \ldots \quad (54)$$

4.1. Uncertainty in α_m

Equation 47 gives the measured position of the neutral axis in terms of surface strain measurements. Applying Equation 54 to Equation 47 gives, after some algebra,

$$\frac{\Delta\alpha_m}{\alpha_m} = 2\varepsilon_{tb}\left[\frac{1}{1-(\varepsilon_{tb}/\varepsilon_{cu})^2}\left(\frac{\Delta\varepsilon_{cu}}{\varepsilon_{cu}}\right)^2 + \frac{1}{(\varepsilon_{cu}/\varepsilon_{tb})^2-1}\left(\frac{\Delta\varepsilon_{tb}}{\varepsilon_{tb}}\right)^2\right]^{1/2} \quad (55)$$

which shows that the uncertainty in α_m depends also on the actual magnitude of the surface strains. Fig. 3 shows the predicted uncertainty in α_m as a function of the measured surface strain ratio $\varepsilon_{cu}/\varepsilon_{tb}$ for two cases of surface tensile strains: $\varepsilon_{tb} = 1$ and 5%. In this calculation, we assumed that the uncertainties in surface strains are 1%. These curves show that the uncertainty in α_m rises rapidly as $\varepsilon_{cu}/\varepsilon_{tb} \to 1$ as would be expected. However, the magnitude of the uncertainties even at surface strain ratios close to unity is less than 0.1%. Thus, under most circumstances, the neutral axis position can be measured accurately.

4.2. Uncertainties in measured elastic modulus

We calculated the uncertainties in the composite facing elastic modulus for the strong and the weak core material. For the strong core material case, we used Equation 49 and applied Equation 54 to obtain, after, considerable algebra, an expression for the uncertainty in E_c, which is

$$\frac{\Delta E_c^2}{E_c^2} = \frac{1}{A^2B^2} \times \Bigg(\{[-8fH(H-2t) + 12t^2 - 24Ht]B - 12t^2A\}^2 \varepsilon_{cu}^2\left(\frac{\Delta\varepsilon_{cu}}{\varepsilon_{cu}}\right)^2 + \{[8fH(H-2t) + 12t^2]B + (12t^2 + 24Ht)A\}^2 \varepsilon_{tb}^2\left(\frac{\Delta\varepsilon_{tb}}{\varepsilon_{tb}}\right)^2 + \{[-32fH(\varepsilon_{tb}-\varepsilon_{cu}) + 24t(\varepsilon_{tb}+\varepsilon_{cu}) - 24H\varepsilon_{cu}]B - [24t\varepsilon_{cu} - 24(H+t)\varepsilon_{tb}]A\}^2 t^2 \times\left(\frac{\Delta t}{t}\right)^2 + \{[16f(H-2t)(\varepsilon_{tb}-\varepsilon_{cu}) - 24t\varepsilon_{cu}]B + 24tA\varepsilon_{tb}\}^2 H^2\left(\frac{\Delta H}{H}\right)^2\Bigg) \quad (56)$$

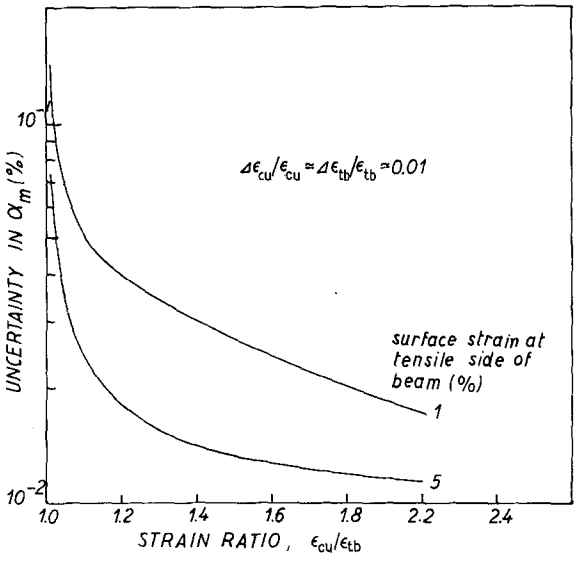

Figure 3 Predicted uncertainty in the measured position of the sandwich beam neutral axis.

where

$$A = [8fH(H - 2t)(\varepsilon_{tb} - \varepsilon_{cu}) + 12t^2(\varepsilon_{tb} + \varepsilon_{cu}) - 24Ht\varepsilon_{tb}] \quad (57)$$

$$B = [12t^2(\varepsilon_{cu} - \varepsilon_{tb}) - 24Ht\varepsilon_{tb}] \quad (58)$$

Fig. 4 shows the predicted uncertainty obtained with Equation 56 using the following numerical values: $t = 0.05H$, $H = 1$ (no specified units), $f = 0.8$ (core stiffness 80% of the stiffness of upper facing or $0.8E_m$), $\Delta t/t \simeq \Delta H/H \simeq 0.01$, and $\Delta\varepsilon_{cu}/\varepsilon_{cu} \simeq \Delta\varepsilon_{tb}/\varepsilon_{tb} \simeq 0.01$. The uncertainty $\Delta E_c/E_c$ is plotted as a function of the surface strain ratio, which shows that the composite elastic modulus can be measured using Equation 49 to an uncertainty of 6% or less depending on the relative stiffness of the top and bottom facings in the sandwich beam. The greater this difference or as E_c/E_m increases, it translates into a greater measured surface strain ratio $\varepsilon_{cu}/\varepsilon_{tb}$ and, hence, lower uncertainty in E_c. However, the limit appears to be around 3% in the uncertainty of E_c for $\varepsilon_{cu}/\varepsilon_{tb} \simeq 2.2$. The curve of Fig. 4 is valid for $0.01 \leqslant \varepsilon_{tb} \leqslant 0.5$ as they all fall in the same place.

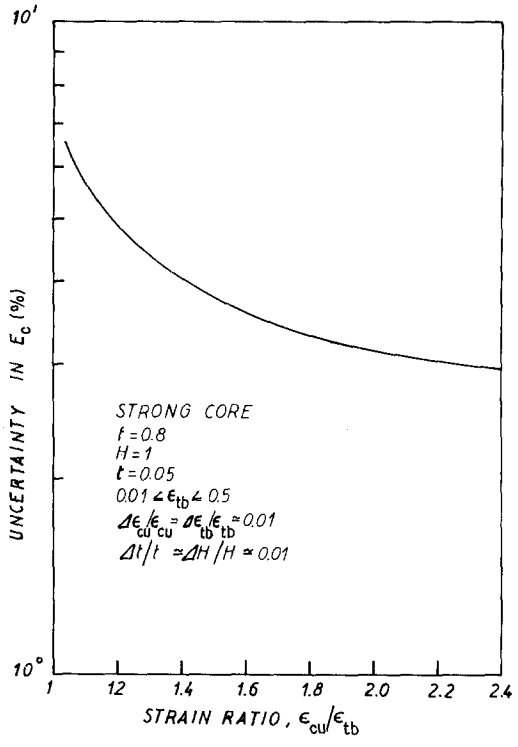

Figure 4 Predicted uncertainty in the measured composite elastic modulus. Strong core case.

The uncertainty in the measurement of E_c for the weak core material was obtained in a similar manner. Equation 54 was applied to Equation 51 to yield, after much algebra,

$$\frac{\Delta E_c^2}{E_c^2} = \frac{16H^2(H - t)^2\varepsilon_{tb}^2\varepsilon_{cu}^2}{[(2H - t)\varepsilon_{tb} - t\varepsilon_{cu}]^2[(2H - t)\varepsilon_{cu} - t\varepsilon_{tb}]^2}\left[\left(\frac{\Delta\varepsilon_{cu}}{\varepsilon_{cu}}\right)^2 + \left(\frac{\Delta\varepsilon_{tb}}{\varepsilon_{tb}}\right)^2\right] + \frac{(\varepsilon_{cu}^2 - \varepsilon_{tb}^2)t^2}{[(2H - t)\varepsilon_{tb} - t\varepsilon_{cu}]^2[(2H - t)\varepsilon_{cu} - t\varepsilon_{tb}]^2}\left\{\left[(2H - t) + \frac{\varepsilon_{cu}^2 + \varepsilon_{tb}^2}{\varepsilon_{cu}^2 - \varepsilon_{tb}^2}\right]\left(\frac{\Delta t}{t}\right)^2 + 4H^2\left(\frac{\Delta H}{H}\right)^2\right\} \quad (59)$$

Fig. 5 shows the predicted uncertainty obtained from Equation 59 using the following numerical values: $t = 0.05H$, $H = 1$ (no specified units), $\Delta t/t \simeq \Delta H/H \simeq 0.01$, and $\Delta\varepsilon_{cu}/\varepsilon_{cu} \simeq \Delta\varepsilon_{tb}/\varepsilon_{tb} \simeq 0.01$. Two cases are shown: measured surface tensile strains of 1 and 5%. As the surface strain values increase, the uncertainty diminishes. Thus, the uncertainty in E_c ranges from 4% down to 1.6%. At values of ε_{tb} greater than 5% the uncertainty in E_c asymptotically approaches 1.5%.

These results show that the weak core material affects the uncertainty as the loading strains increase, meaning that uncertainties in E_c are best estimated at high elastic strains. The uncertainty in E_c also sharply increases with the surface strain ratio at low tensile strains. These effects are consequences of the models developed in this paper.

4.3. Uncertainties in measured values of V_f

For the case of a strong core material, Equation 54 is applied to Equation 52 which yields, after much algebra, the uncertainty in the measured fibre volume fraction, or

$$\frac{\Delta V_f^2}{V_f^2} = \frac{1}{AB^2(\varepsilon_{tb} - \varepsilon_{cu})^2}\left\{[-B - 3(K_0 - 1) \times (\varepsilon_{tb} - \varepsilon_{cu})t]^2\varepsilon_{cu}^2\left(\frac{\Delta\varepsilon_{cu}}{\varepsilon_{cu}}\right)^2 + \{B - (\varepsilon_{tb} - \varepsilon_{cu}) \times [3(K_0 - 1)t - 2H]\}^2\varepsilon_{tb}^2\left(\frac{\Delta\varepsilon_{tb}}{\varepsilon_{tb}}\right)^2\right\} + \frac{1}{A^2B^2} \times \left(\{(-8fH^2/2t^2)B - A[3(K_0 - 1)\right.$$

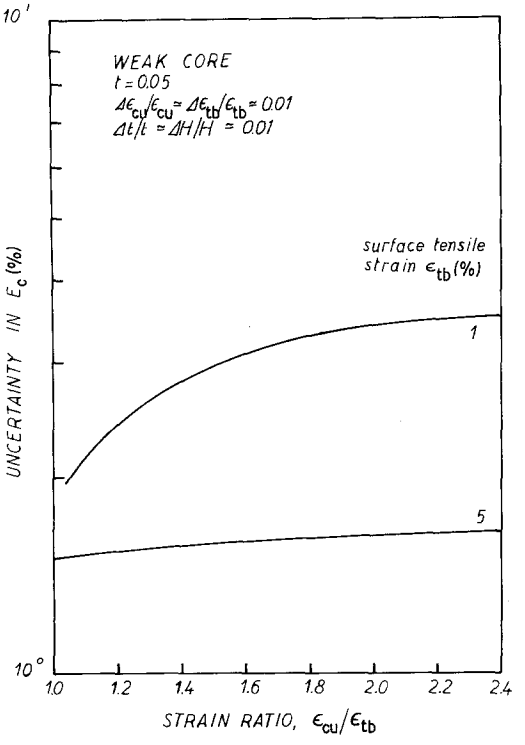

Figure 5 Predicted uncertainty in the measured composite elastic modulus. Weak core case.

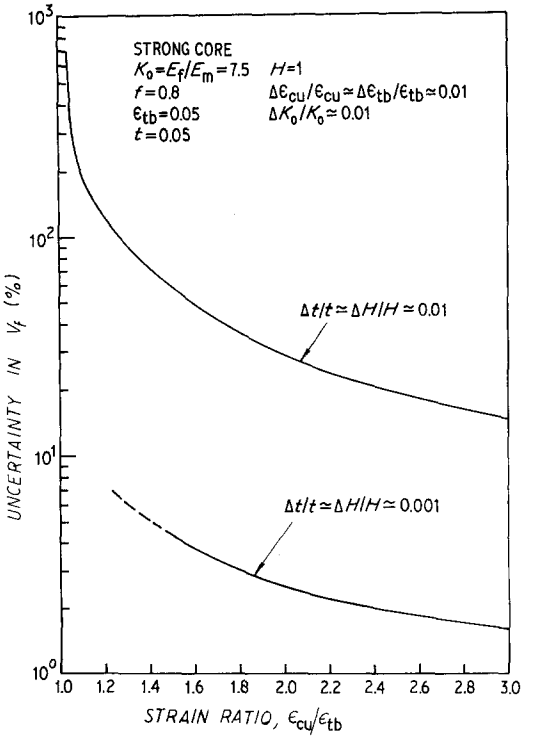

Figure 6 Predicted uncertainty in the measured composite fibre volume fraction. Strong core case.

$$\times (\varepsilon_{cu} + \varepsilon_{tb})]\}^2 t^2 \left(\frac{\Delta t}{t}\right)^2 + \{[8f(H/2t - 1) + 6]B + 6A(K_0 - 1)\varepsilon_{tb}\}^2 H^2 \left(\frac{\Delta H}{H}\right)^2 \Big) - \frac{9}{B^2}[(\varepsilon_{cu} + \varepsilon_{tb})t - 2H\varepsilon_{tb}]^2 K_0^2 \left(\frac{\Delta K_0}{K_0}\right)^2 \quad (60)$$

where

$$A = [8fH(H/2t - 1) + 6H](\varepsilon_{tb} - \varepsilon_{cu}) \quad (61)$$

$$B = 3(K_0 - 1)[(\varepsilon_{cu} + \varepsilon_{tb})t - 2H\varepsilon_{tb}] \quad (62)$$

Fig. 6 shows a plot of the predicted uncertainties in V_f as a function of the surface strain ratio. These results were obtained with the following numerical values: $K_0 = 7.5$ (ratio of graphite fibre to aluminium matrix elastic modulus), $t = 0.05\,H$, $H = 1$ (no specified units), $f = 0.8$ (core material has 80% of the top facing stiffness or $0.8\,E_m$), $\Delta\varepsilon_{cu}/\varepsilon_{cu} \simeq \Delta\varepsilon_{tb}/\varepsilon_{tb} \simeq 0.01$, and $\Delta K_0/K_0 \simeq 0.01$. Two curves are shown in Fig. 6: one for an uncertainty in the dimension of the sandwich beam of $\Delta t/t \simeq \Delta H/H \simeq 0.01$, and one for $\Delta t/t \simeq \Delta H/H \simeq 0.001$. The prediction of V_f for a strong core, while generally decreasing sharply with an increased ratio of surface strains, appears very sensitive to the uncertainty in measured beam dimensions. Therefore, if this method were used to determine the fibre volume fraction in the composite, the values of t and H must be measured to an uncertainty better than 0.001 to obtain uncertainties in V_f less than about 4 to 5%.

A similar analysis was carried out for the case of a very weak core using Equation 53 into Equation 54. The results, after much algebra, give

$$\frac{\Delta V_f^2}{V_f^2} = \frac{4(K_0 - 1)^2}{[(2 - K_0)\varepsilon_{cu} - K_0\varepsilon_{tb}]^2 (\varepsilon_{tb} - \varepsilon_{cu})^2} \times \left\{\varepsilon_{cu}^4 \left(\frac{\Delta\varepsilon_{cu}}{\varepsilon_{cu}}\right)^2 + \varepsilon_{tb}^4 \left(\frac{\Delta\varepsilon_{tb}}{\varepsilon_{tb}}\right)^2 + [(2\varepsilon_{cu} + \varepsilon_{tb})^2 \times (\varepsilon_{tb} - \varepsilon_{cu})^2] K_0^2 \left(\frac{\Delta K_0}{K_0}\right)^2\right\} + \frac{(t/H)^2}{(1 - t/H)^2}\left[\left(\frac{\Delta t}{t}\right)^2 + \left(\frac{\Delta H}{H}\right)^2\right] \quad (63)$$

Fig. 7 shows a plot of Equation 63 for the following numerical values: $K_0 = 7.5$,

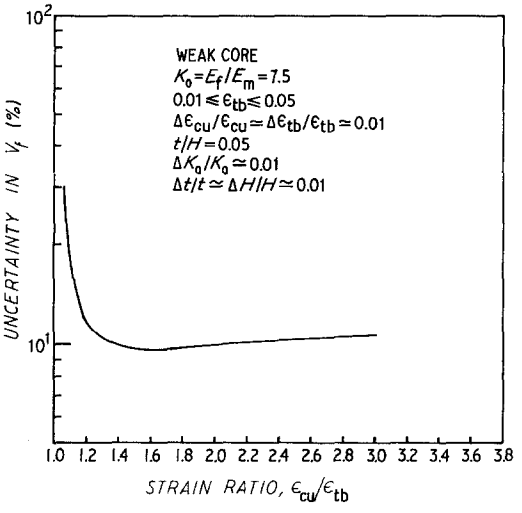

Figure 7 Predicted uncertainty in the measured composite fibre volume fraction. Weak core case.

$0.01 \leqslant \varepsilon_{tb} \leqslant 0.05$, $t/H = 0.05$, $\Delta K_0/K_0 \simeq 0.01$, $\Delta t/t = \Delta H/H \simeq 0.01$, and $\Delta\varepsilon_{cu}/\varepsilon_{cu} \simeq \Delta\varepsilon_{tb}/\varepsilon_{tb} \simeq 0.01$. This figure shows that the uncertainty in V_f for a sandwich beam with a weak core material drops off very rapidly with increasing surface strain ratio to a minimum value of about 10% at $\varepsilon_{cu}/\varepsilon_{tb} \simeq 1.6$ and rises very slowly thereafter. Thus, in this case, the value of V_f cannot be obtained to a better uncertainty than about 10%. Schoutens [5] has shown elsewhere that the volume fraction of composite materials can be obtained with an uncertainty of 0.5% using a simple laboratory balance with a precision of 0.01% provided the composite contains no porosity. If porosity is present, the uncertainty is around 3% by that method [5].

Finally, we have seen that the compressive or tensile strain in any layer within the beam is given by Equation 39 or 40. Applying Equation 54 yields the following expression for the uncertainty in the compressive strain measurements

$$\left(\frac{\Delta\varepsilon_c}{\varepsilon_c}\right)^2 = \left(\frac{\Delta y}{y}\right)^2 + \left(\frac{\Delta H}{H}\right)^2 + \left(\frac{\Delta\varepsilon_{cu}}{\varepsilon_{cu}}\right)^2 + \left(\frac{\Delta\alpha}{1+\alpha}\right)^2 \quad (64)$$

and for the tensile strain measurements

$$\left(\frac{\Delta\varepsilon_t}{\varepsilon_t}\right)^2 = \left(\frac{\Delta y}{y}\right)^2 + \left(\frac{\Delta H}{H}\right)^2 + \left(\frac{\Delta\varepsilon_{tb}}{\varepsilon_{tb}}\right)^2 + \left(\frac{\Delta\alpha}{1+\alpha}\right)^2 \quad (65)$$

Assuming as above that $\Delta y/y \simeq \Delta H/H \simeq 0.01$, using $\Delta\varepsilon_{cu}/\varepsilon_{cu} \simeq \Delta\varepsilon_{tb}/\varepsilon_{tb} \simeq 0.01$, and assuming from the above analysis that $\Delta\alpha/(1 \pm \alpha) \simeq \Delta\alpha/\alpha \simeq 0.005$, then $\Delta\varepsilon_t/\varepsilon_t \simeq \Delta\varepsilon_c/\varepsilon_c \simeq 0.018$ or 1.8%. In the analysis of the uncertainties in α_m, E_c, and V_f, we have used $\Delta\varepsilon_{tb}/\varepsilon_{tb} \simeq \Delta\varepsilon_{cu}/\varepsilon_{cu} \simeq 0.01$ rather than 0.018 for illustration of trends in measurements. Using the latter value (0.018) would not have altered the results significantly.

References

1. C. W. BERT, *J. Mater. Sci. Lett.* **1** (1982) 247.
2. C. ZWEBEN, W. S. SMITH and M. W. WARDLE, "Test Methods for Fiber Tensile Strength, Composite Flexural Modulus, and Properties of Fabric-Reinforced Lamines", Composite Materials: Testing and Design (Fifth Conference) ASTM STP 674 (American Society for Testing and Materials, Philadelphia, 1979) p. 228.
3. J. E. SCHOUTENS, unpublished data.
4. S. TIMOSHENKO, "Strength of Materials", Part I – Elementary Theory and Problems. 3rd Edn (Van Nostrand, New York, 1955) p. 218.
5. J. E. SCHOUTENS, *J. Mater. Sci.* **19** (1984) 957.

Received 13 December 1984
and accepted 15 January 1985